Mechanically Reconfigurable Linear Phased Array Antenna Based on Single-Block Waveguide Reflective Phase Shifters With Tuning Screws

LUCAS POLO-LÓPEZ[1], **JOSÉ LUIS MASA-CAMPOS**[1],
ALFONSO TOMÁS MURIEL-BARRADO[1,2], **PABLO SANCHEZ-OLIVARES**[2],
EDUARDO GARCIA-MARIN[1], **JUAN CÓRCOLES**[1], (Senior Member, IEEE),
AND JORGE A. RUIZ-CRUZ[1], (Senior Member, IEEE)

[1]Escuela Politécnica Superior, Universidad Autónoma de Madrid, 28049 Madrid, Spain
[2]Escuela Técnica Superior de Ingenieros de Telecomunicación, Universidad Politécnica de Madrid, 28040 Madrid, Spain

Corresponding author: Lucas Polo-López (lucas.polo@estudiante.uam.es)

ABSTRACT This work presents the design and prototyping of a reconfigurable phased array in Ku band (16 to 18 GHz) implemented in waveguide technology. The design is based on the use of a novel seamless waveguide module integrating four reconfigurable phase shifters to adjust the relative phase shift between the unitary elements of a linear array, which are illuminated uniformly by a corporate waveguide feeding network. The phase shifters are implemented by a 90° hybrid coupler in waveguide technology where two of its ports are loaded with a tunable reactive load, implemented in this proof of concept with a tuning screw. The four phase shifters have been manufactured in a single part using direct metal laser sintering, avoiding the losses related to bad electric contacts and misalignments associated to multipart devices. This also simplifies the assembly of the full phased array, leading to a modular approach with three parts whose design can be addressed separately. The experimental results for the complete array antenna show great performance and demonstrate that the main-lobe of the radiation pattern can be effectively scanned continuously between the angles −25° and 25°, with a high efficiency in the whole design band thanks to the proposed waveguide implementation.

INDEX TERMS Beam steering, couplers, phased arrays, phase shifters.

I. INTRODUCTION

In the last years different reconfiguration techniques have been developed in the area on antenna systems in order to increase their flexibility. The scanning of the radiation pattern main lobe, which is one of these techniques, has been extensively applied to planar array antennas by using tunable electronic components like varactor diodes, p-i-n diodes or digital phase shifters [1]–[5]. These components, which have been used by some of the authors in previous works [6], [7], allow a fast reconfiguration of the array characteristics but,

The associate editor coordinating the review of this manuscript and approving it for publication was Davide Comite[ID].

as a counterpart, produce high levels of insertion losses. A recent alternative to varactor or p-i-n diodes is the use of functional materials to create reconfigurable antennas. The main advantage of these new materials over tunable electronic elements is that they can be used in higher frequency designs [8]–[11].

Regarding the power losses and radiation efficiency, a better alternative is the use of waveguide antenna arrays. In the recent years some advances have been made in the integration of tunable electronic components with waveguide devices [12]–[15], although there is still margin for improvement. On the other hand, while presenting a longer reconfiguration time than the electronic alternatives, mechanical

reconfiguration techniques are specially adequate to achieve high performance and low power losses [16]–[18].

In this field, Tuning Screws (TS) have been extensively used in the last decades to tune filters [19] or to implement reconfigurability in waveguide devices [20], [21]. Recently, this technique has been proposed by the authors to implement reconfiguration in waveguide array antennas [22]–[24] achieving satisfactory results in terms of radiation efficiency, power losses and scanning performance.

In [24] a linear array antenna fed by a corporate waveguide network was presented. Thanks to the insertion of TS in the feeding network, the phase of the signal at each of the outputs could be controlled producing therefore a scan of the radiation pattern. To control a four element array antenna, 43 TS had to be adjusted. Different configurations (depending on whether each TS was inserted or removed in the waveguide) were defined, each of them producing a certain progressive phase shift between the array elements. Therefore the realized beam-scanning was non-continuous.

In this work, instead of directly inserting TS in the feeding network, a novel Waveguide Reflection-type Phase Shifter (WRPS) is introduced between each of the network outputs and its corresponding array element. These phase shifters, which use a very compact topology, include a pair of TS that allow to adjust the phase shift between its input and output ports. Therefore the progressive phase shift that produces the beam scan can be controlled by tuning each of these phase shifters. Moreover, the WRPS can be manufactured in a single part by additive manufacturing with selective laser sintering, reducing the number of interfaces and providing a compact integration with the other elements of the antenna array. These features will be exploited in an array operating at Ku band, at which different satellite services are allocated. More specifically at the exact operation band of the device (16 to 18 GHz) the European Conference of Postal and Telecommunications Administrations defines several sub-bands for Fixed Satellite Service and Earth observation [25].

The approach introduced in this paper benefits from the inherent advantages of waveguide antennas like high efficiency, low losses and high power handling capabilities. In addition, it presents two important advantages over the design in [24]. First, the progressive phase shift between array elements can be adjusted continuously, enabling to scan the radiation pattern main beam to any desired direction instead of fixed values. Second, it will be shown that each WRPS is adjusted using only two TS, which significantly reduces the number of TS of the whole antenna array (8 instead of 43) while still achieving the same beam scanning range.

II. CONFIGURATION OF THE ANTENNA ARRAY

The designed reconfigurable antenna array, depicted in Fig. 1, consists of a four element linear Aperture Stacked Patch Array (ASPA) fed by a Corporate Waveguide Feeding Network (CWFN). Between each of the outputs of the CWFN and its corresponding radiating element of the ASPA,
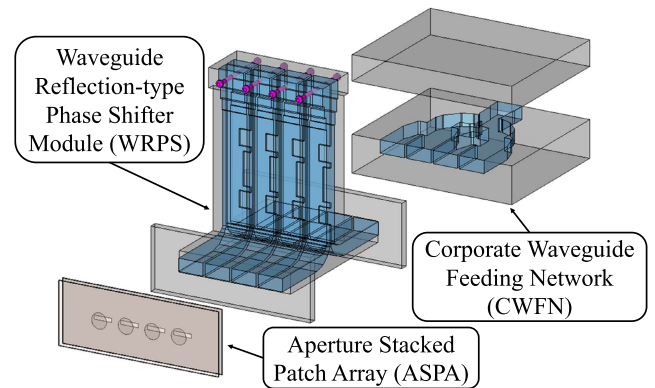
FIGURE 1. Representation of the different parts that compose the proposed phased array. The eight Tuning Screws (TS) of the Waveguide Reflection-type Phase Shifter (WRPS) module (integrating four phase shifters that will be manufactured in a seamless part) are highlighted in magenta at the top of the structure.

a Waveguide Reflection-type Phase Shifter (WRPS), completely implemented in waveguide technology, is inserted.

The CWFN, introduced in [26], follows an H-plane configuration and has one input and four output ports, all of them in WR51 standard waveguide ($a = 12.95$ mm, $b = 6.48$ mm). This device divides the signal at its input port between the four output ports with equal amplitude and phase. For the prototype presented in this work, the CWFN has been manufactured by means of conventional Computer Numerical Control (CNC) machining in two parts. The inner cavities of the waveguides have been machined on an aluminium block which is covered by a flat aluminium slab (as it can be seen in Fig. 1). Both parts are joined together by means of several assembling screws in order to guarantee a good electrical contact between them (for the sake of visualization, the holes corresponding to these screws are not represented in Fig. 1).

The ASPA consists of two substrate layers separated by a Rohacell foam layer with $\varepsilon_r = 1.05$. On one of the substrate layers an array of circular patches is engraved. Each of these patches, whose design is described in [27], is stacked over a radiating slot engraved on the other substrate layer. These slots are excited by the outputs of the WRPS module. The spacing between the array elements is $0.8\lambda_0$, which is meant to produce a beamwidth at -3 dB of $17°$ in the scanning plane. These elements have been distributed as close as possible taking into account the width of the WR51 outputs and that the wall between adjacent outputs should have a thickness of 1 mm so that the CWFN could be machined. It must be highlighted that although the use of dielectric parts could be considered as not compatible with aerospace applications, the presented ASPA could be replaced by other radiating structures such as cavity slots at the end of the waveguide outputs [22]. However in the presented prototype this substrate based array has been used since the authors were interested in providing reconfiguration capabilities to the design in [26].

The WRPS module is composed of four independent WRPS. Each of the WRPS presents two TS which, as it will be seen later, allow to modify the phase shift between the input and output ports of the device depending on how deep the screws penetrate in the waveguide. By adjusting each phase shifter in the WRPS module the relative phase shift between the array elements can be controlled, producing the consequent scanning of the radiation pattern. It is worth mentioning that the presented prototype must be taken as a proof of concept. In a final implementation of the device for operating in a real system the TS could be replaced by fully automated adjustable posts controlled electronically as is [28], [29].

It must be emphasized that although the present array only uses four radiating elements this number could be easily augmented. Increasing the amount of radiating elements in the ASPA is straightforward, as well as increasing the number of stacked phase shifters in the WRPS module. It would only be necessary to design a CWFN with a number of output ports according to the number of radiating elements.

III. SINGLE-BLOCK MODULE FOR THE RECONFIGURABLE PHASE SHIFTERS

The WRPS is one of the most important parts of the presented reconfigurable phased array since it controls the scanning of the radiation pattern. This device is based on the concept of the reflection-type phase shifter [30, Ch. 11], which consists in loading the transmitted and coupled ports of a 90° hybrid with an adjustable reactive load. The resulting two port device behaves as a phase shifter whose phase shifting value depends on the value of the reactive load.

This topology has been exploited extensively in planar circuitry using tunable electronic elements like varactor or p-i-n diodes to implement reflection-type phase shifters [3], [4], [31]. However, printed circuits are not recommended for some applications, like space communications, with special requirements like high power handling, very low power losses and materials that can handle very extreme pressure and temperature conditions.

In this work a waveguide 90° hybrid coupler where two of its ports are loaded by a tunable reactive load completely implemented in waveguide technology [32], [33] is proposed. This load consists of a short-circuited waveguide section where a TS is inserted. The reactance of the loads (and consequently the phase shift between the input and output ports of the WRPS) is controlled by adjusting how much the screw penetrates in the waveguide (parameter h in Fig. 2). It should be noted that this allows for a continuous (i.e. not restricted to discrete values) control of the realised phase shift.

Different kinds of waveguide structures can be used to implement the 90° hybrid coupler part of the WRPS. For example, the Riblet short-slot hybrid junction is known to produce a very compact device [34], [35] and it was indeed used by the authors in a previous work [32]. Other alternatives can provide better performance (in terms of bandwidth) [36],
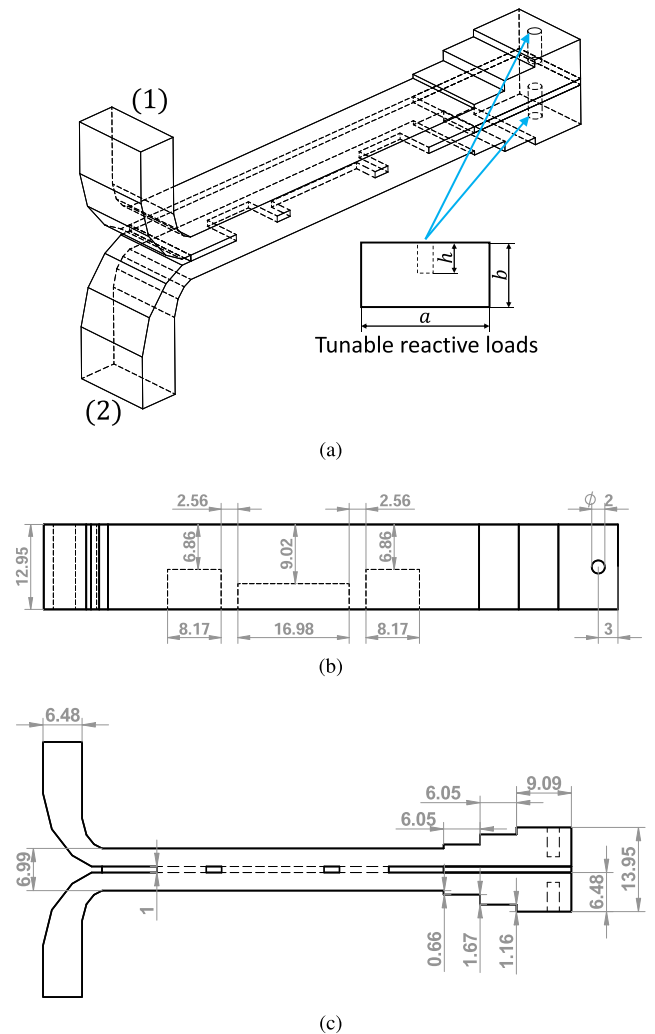

FIGURE 2. Representation of a single Waveguide Reflection-type Phase Shifter (WRPS) based on a 90° hybrid coupler with ports in *E*-plane configuration and with a profiled metallic septum inside the structure. (a) 3D view and detail of the tunable reactive load (piece of short-circuited waveguide with a metallic post implemented with a tuning screw) terminating two ports of the coupler. (b) Top view with annotations for the main dimensions. (c) Lateral view with annotations for the main dimensions.

as is the case of the coupler used in the present work. A representation of the designed WRPS can be found in Fig. 2.

For manufacturing the prototype of the antenna array, four WRPS had to be mounted next to each other between the CWFN and the ASPA. The combination of the four WRPS is the WRPS module in Fig. 1. It must be noticed that the allowed spacing between the four WRPS was given by the spacing between unitary elements of the ASPA (as was described in Section II).

The manufacturing of the WRPS module by means of classic techniques (splitting the device in several parts which can be machined by CNC milling) would have been very complex since there would not be enough space to place the required number of assembling screws to guarantee a good electrical contact between all the parts. Therefore an additive
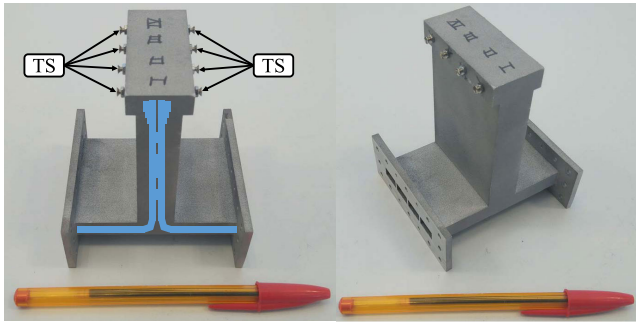
FIGURE 3. Photographs of the Waveguide Reflection-type Phase Shifter (WRPS) module integrating four phase shifters in a seamless part manufactured by Direct Metal Laser Sintering (DMLS). The layout of the phase shifters (as in Fig. 2) is represented in blue over the photograph in the left. The tuning screws (TS) are at the top of the structure.

manufacturing approach was chosen since it allowed to build the device in a single piece. More specifically a Direct Metal Laser Sintering (DMLS) technique was used, avoiding the metallization of the built device (as it is usual with other plastic based additive manufacturing techniques) since the used building material is metallic [37]. A photograph of the prototype can be found in Fig. 3.
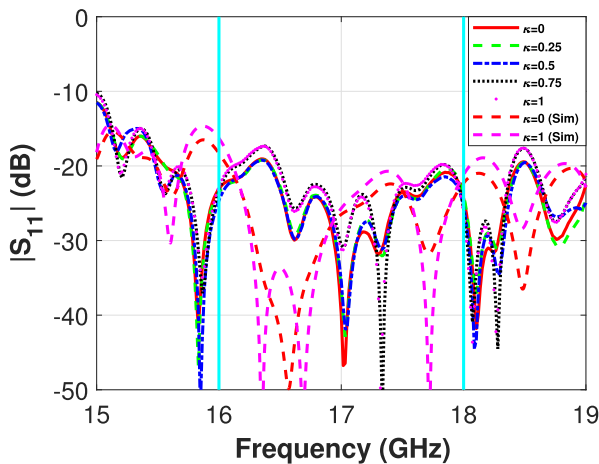
FIGURE 4. Measured and simulated magnitude of the S_{11} parameter of one of the phase shifters in the WRPS module (the one labelled as IV in Fig. 3) for different configurations of the tuning screws (different normalized penetration length κ). The results for the other phase shifters of the module are omitted since they are identical.

Although it would have been possible to manufacture the CWFN and the WRPS module in a single part it was preferred to build the WRPS module in a separate part in order to be able to measure experimentally the scattering parameters of each phase shifter independently. Fig. 4 and Fig. 5 show, respectively, the magnitude of the S_{11} parameter and the magnitude and phase of the S_{21} parameter, both of them measured experimentally in the built prototype for different configurations of the TS. The parameter κ represents the screw penetration in the short-circuited waveguide, h, normalized to the waveguide height, b (i.e. $\kappa = h/b$) as in Fig. 2. The low S_{11} level in Fig. 4 ($|S_{11}| < -17$ dB

(a)

(b)
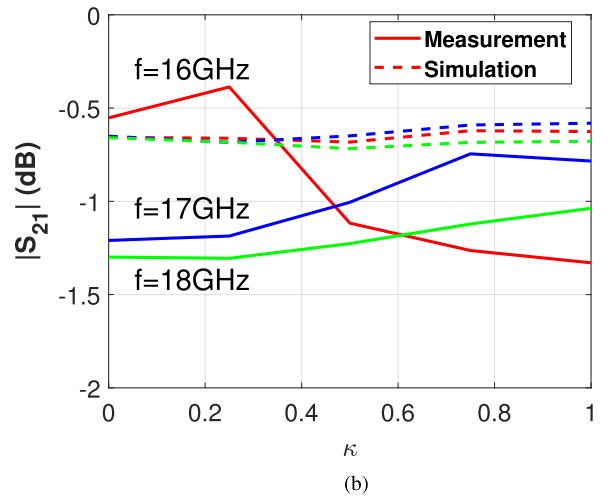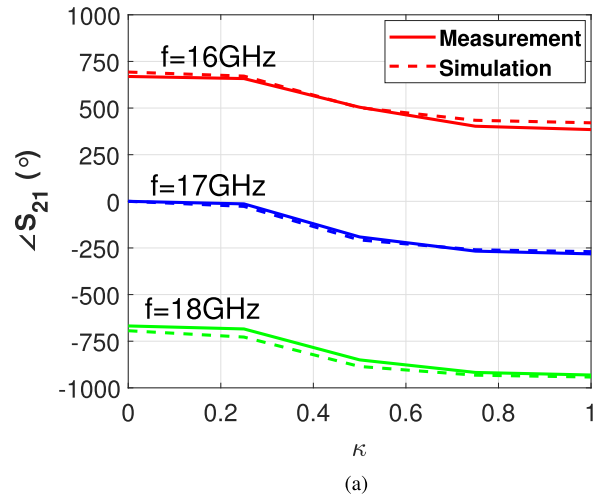
FIGURE 5. Measured and simulated (a) phase and (b) magnitude (at different frequencies) of the S_{21} parameter produced by one of the phase shifters in the WRPS module (the one labelled as IV in Fig. 3) for different configurations of the tuning screws (different normalized penetration length κ). The results for the other phase shifters of the module are omitted since they are identical.

for the whole operation band) anticipates that the WRPS module will not disturb the original array behaviour when it is integrated with the rest of the components. The small discrepancies in the nulls position between the simulated and measured values in Fig. 4 are explained by the experimental condition of the DMLS technique. However, since the measured and simulated reflection coefficient level is the same (and below -17 dB) it can be considered that the results are satisfactory.

The most important parameter in order to asses the performance of the device is the achieved phase shifting range (i.e. $\angle S_{21}\rfloor_{\kappa=0} - \angle S_{21}\rfloor_{\kappa=1}$), since this will directly impact the beam scanning range that can be achieved by the array. For the proposed WRPS, a phase shifting range of 270° is achieved at the central frequency ($f_0 = 17$ GHz). As it will be shown, this phase shifting range is enough to adequately scan the main lobe of the radiation pattern produced by the array. If necessary, the phase shifting range could be increased by placing the TS closer to the short-circuit [32]. For this specific

design this range could have been increased up to 310° by placing the screw at 0.5 mm of the short-circuit. However, it must be noted that increasing the phase shifting range also increases the tuning sensitivity since for the same variation of h the change in the phase shift will be higher. Therefore, in order to ease the tuning process, it is preferred to design the phase shifter to present the minimum phase shifting range necessary to adequately scan the array radiation pattern.

Finally, the insertion losses observed in Fig. 5 (b) are mostly due to the conductivity of the material used to build the phase shifters and the rough finish of the waveguide walls inherent to the DMLS process. However, given the novelty of this manufacturing technique the obtained experimental results can be considered successful. The differences between the measured and simulated values are caused by the difficulty in making a proper estimation of the manufacturing material conductivity.

TABLE 1. Comparison of the ratio between the phase shifting range achieved by the design proposed in this work and other works in the state of the art.

Parameter	This work	[3]	[33]
Phase shifting range (°)	270	370*	180
Central frequency (GHz)	17	12.5	92.5
Insertion loss (dB)	1.2	1.5	0.6
Phase shift per insertion loss (°/dB)	225	247	300
Technology	Waveguide	Planar	Waveguide
Complexity	Medium	Medium	High

*This phase shifting range is achieved thanks to the combined use of three hybrid couplers.

An interesting figure of merit for these kind of devices consists in computing the ratio of the achieved phase shifting range and the insertion losses. For the proposed phase shifter this produces a result of 225°/dB. This value is compared with other state-of-the-art works in Table 1. It must be emphasized that the design in [3] achieves such a high phase shifting range thanks to the use of three 90° hybrid couplers and, in addition, its implementation in planar technology limits it applicability to higher frequency bands. Regarding the design in [33], the lower insertion losses in comparison with the proposed design are explained by the manufacturing using conventional machining instead of DMLS. As shown by [32], if the phase shifter presented in this work were manufactured using conventional machining the obtained insertion losses would be lower.

IV. ARRAY ANTENNA INTEGRATION AND EXPERIMENTAL RESULTS

A photograph of the complete antenna, along with detailed views of the CWFN and the ASPA can be found in Fig. 6.
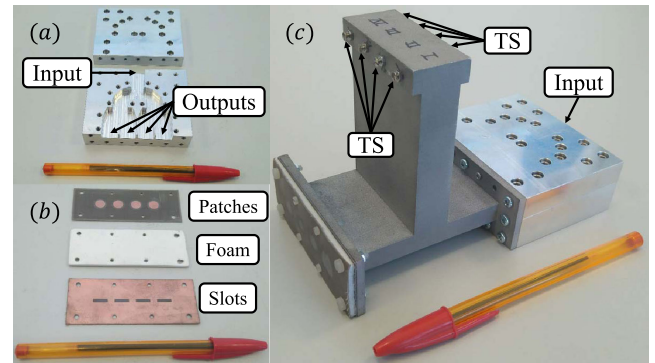
FIGURE 6. (a) Corporate Waveguide Feeding Network (CWFN), (b) Aperture Stacked Patch Array (ASPA), (c) Complete phased array antenna, assembling in a very compact layout the three parts: CWFN, WRPS and ASPA.

In these pictures the different manufacturing techniques employed to build each of the antenna parts can be appreciated: CNC machining for the CWFN, planar technology for the ASPA and DMLS for the WRPS module.

TABLE 2. Phase shift (in degrees) produced by each of the phase shifters in the WRPS module for different scanning directions (θ_0).

		Ideal			Measured		
θ_0	α	$\alpha_2 - \alpha_1$	$\alpha_3 - \alpha_1$	$\alpha_4 - \alpha_1$	$\alpha_2 - \alpha_1$	$\alpha_3 - \alpha_1$	$\alpha_4 - \alpha_1$
0	0	0	0	0	358.25	358.83	0.03
5	25.10	25.10	50.20	75.30	26.00	48.00	74.30
10	50.01	50.01	100.02	150.03	49.08	105.04	160.64
15	74.54	74.54	149.08	223.62	77.88	153.34	224.01
20	98.50	98.50	197.00	295.51	92.66	200.40	297.11
25	121.71	121.71	243.43	5.14	115.85	246.06	5.49

To demonstrate the scanning capabilities of the array, the radiation pattern has been scanned between $\theta = -25°$ to $\theta = 25°$ with a step of 5°. The radiation pattern has not been scanned further since for a greater scanning angle the level of the grating lobe would be similar to that of the main lobe. Table 2 shows the necessary progressive phase shift (α) for each scanning direction. This table also shows the phase shift that must be introduced by each phase shifter ($\alpha_i, i = 1, \ldots, 4$) of the WRPS module in order to obtain the specified progressive phase shift. It should be noted that Table 2 only considers the positive values of θ_0. In order to scan the radiation pattern to a negative direction, it is enough to reverse the phase shift assigned to each element (i.e. $\alpha_{1,neg} = \alpha_{4,pos}, \alpha_{2,neg} = \alpha_{3,pos}, \alpha_{3,neg} = \alpha_{2,pos}, \alpha_{4,neg} = \alpha_{1,pos}$).

Before measuring the radiation pattern of the antenna, it was interesting to verify that the WRPS module behaved as expected. For this reason a measurement of the phase shift for different scanning directions was performed. The measured phase shift values for each scanning direction are collected in Table 2 and compared with the ideal ones that would produce the exact progressive phase shift. The mean error between the two sets of values is below 2.85°.

The small differences that are observed can be explained by different factors. It must be noted that any asymmetry in the WRPS can affect to the combination of incident and reflected waves in the hybrid coupler and therefore the behaviour of the phase shifter will not be exactly as expected. Two different sources of asymmetry can occur: manufacturing errors and imbalance in the TS. The DMLS technique employed for building the prototype is still quite novel and therefore some errors can occur when building the waveguide device. Unfortunately, due to the monolithic manufacturing it is not possible to check the inner parts of the device without destroying it. On the other hand, since in this initial proof-of-concept prototype the TS are adjusted manually, it is possible that there is an accidental imbalance between both screws that affects the obtained phase shift. In fact, the presented prototype has been created as a proof of concept to demonstrate the feasibility of the design. Nevertheless the manually adjusted TS could be substituted in a later implementation by fully automated sliding posts controlled electromechanically by means of a piezoelectric motor [28], [29]. This would enable the possibility of an automatic reconfiguration and would also increase the precision of the tuning process

Additionally, even if there were no symmetry issues, there is still another source of error related to the tuning resolution. As it was mentioned, the change in the phase shift with respect to the variation of h is continuous and therefore the tuning resolution should be, ideally, infinite. Nevertheless, since the TS are adjusted manually, there is a practical limit on the minimum fraction of turns that can be applied to a screw. In this work it is considered that the finest degree of control that can be achieved in the screw adjusting process is a quarter of turn. Nevertheless, it should be pointed out that these two problems (imbalance of the TS and tuning resolution) would be mitigated in a final implementation of the antenna where the TS are implemented as sliding posts controlled electromechanically [28], [29].

Despite everything of the above, it should be emphasized that the obtained phase shifting errors are so small that, as it will be seen, their effect on the radiation pattern scanning is negligible, especially given the fact that the $-3\,\mathrm{dB}$ beamwidth is $17°$.

It is also important to study the isolation between the different antenna array channels since a low isolation will degrade the radiation pattern produced by the array. Fig. 7 shows the simulated S parameters accounting for the isolations between the four channels of the ASPA combined with the WRPS module. It can be appreciated that the isolation level is higher than $25\,\mathrm{dB}$ for all the channel pairs which guarantees the correct performance of the array. Please note that the isolation values not represented in the figure can be obtained applying the symmetry and reciprocity properties of the structure.

The measured radiation patterns for the different scanning directions have been represented in Fig. 8 (please note that only the *H*-plane cut is represented since it is the one in which the main-lobe is scanned) along with the simulated results. For the case of $\theta_0 = 0°$ the measured radiation pattern is
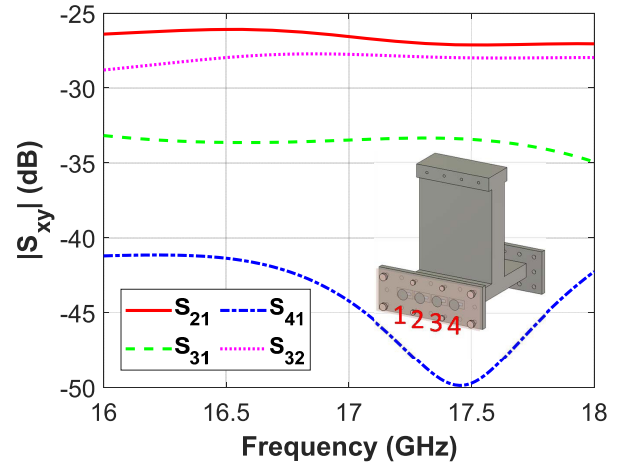

FIGURE 7. Simulated isolation between different channels of the antenna array.
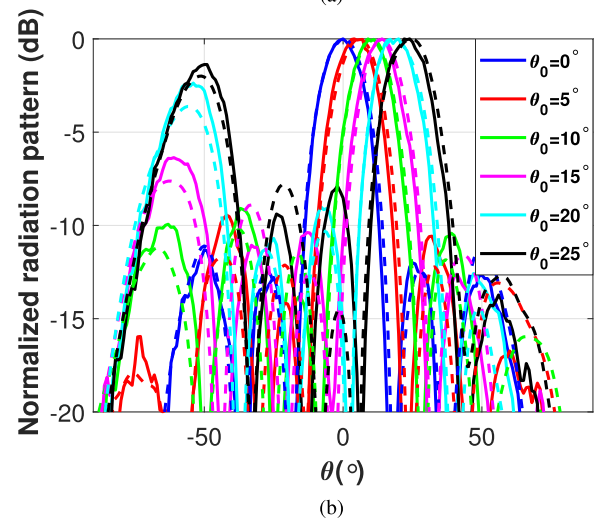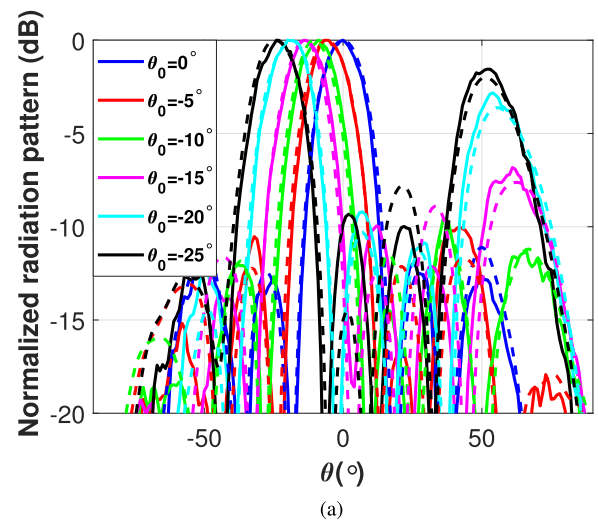

(a)

(b)

FIGURE 8. Measured (solid) and simulated (dashed) *H*-plane radiation pattern for different scanning directions θ_0.

the same that was obtained when measuring the array without the WRPS module [26], which shows that the phase shifters do not introduce a significant disturbance in the behaviour of
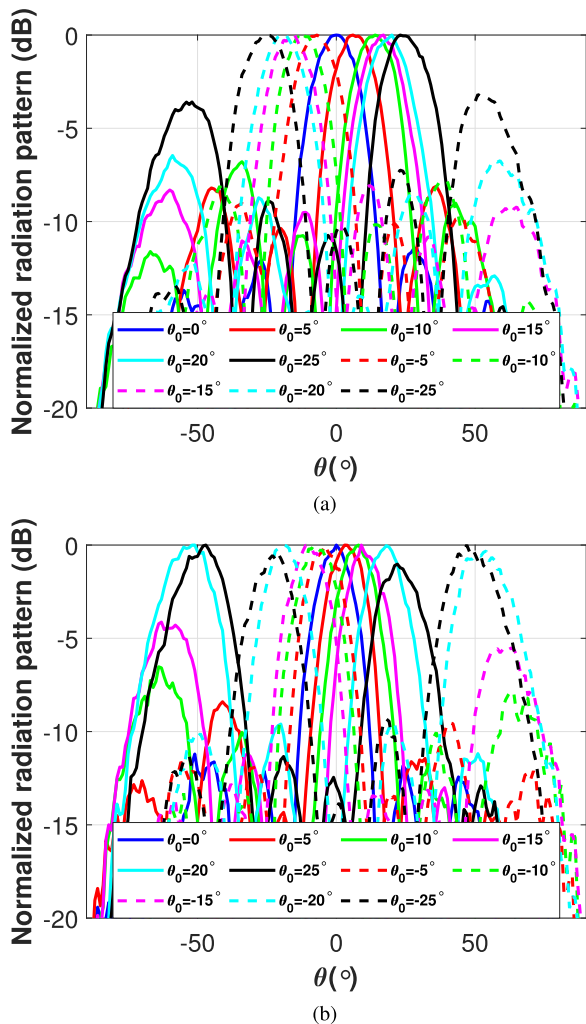
FIGURE 9. Measured *H*-plane radiation pattern for different scanning directions θ_0 at (a) 16 GHz and (b) 18 GHz.

Nevertheless, it is important to emphasize that there is a good correspondence between the experimental and simulated results for all the scanning directions, which demonstrates the reliability of the proposed beam scanning mechanism.
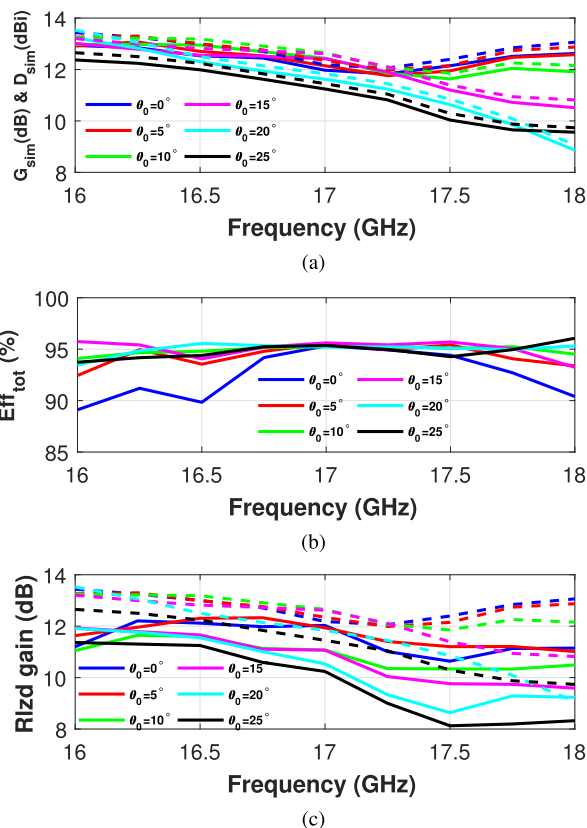

FIGURE 10. (a) Simulated realized gain (G_{sim}, solid) and simulated directivity (D_{sim}, dashed). (b) Total efficiency (G_{sim}/D_{sim}). (c) Measured realized gain (G_{meas}, solid) and simulated realized gain (G_{sim}, dashed).

the antenna. This is in accordance with the scattering parameters measured for a single phase shifter of the WRPS module (shown in Fig. 4), which suggested that this module could be integrated seamlessly in the antenna array. Additionally, Fig. 9 shows the measured radiation pattern at the ends of the operation band (16 GHz and 18 GHz). As it can be appreciated the beam scan is maintained over the whole operation band.

When the scanning angle is increased beyond $|\theta_0| \geq 10°$ a grating lobe appears and the SLL starts degrading very fast. This is in part due to the unitary elements spacing at the ASPA ($0.8\lambda_0$), but it is not possible to make this distance smaller since it is bounded by the width of the waveguide that illuminates each of the elements. One possible solution would be to use a CWFN design with an *E*-plane configuration, which would enable a $0.6\lambda_0$ spacing of the array elements. In this situation it would be necessary to have an WRPS with *H*-plane configuration. This would not suppose a problem since a design of such device has already been proposed by the authors [32].

Additionally, Fig. 10 shows the simulated and measured values of directivity (D_{sim}) and gain (G_{sim}, G_{meas}) for different scanning directions. As it can be appreciated the simulated values for the directivity and the realized gain are very similar, which is in accordance with the high efficiencies typically achieved by waveguide designs thanks to their low power losses. Fig. 10 (c) shows that the measured gain is slightly lower than the simulated one. This can be explained by an effect that is not taken into account in the simulation, which is the electrical contact between the TS and the waveguide walls. Since this contact is not perfect, some of the power transmitted by the waveguide is coupled to the TS (like if the screw were a coupling pin [38], [39]) and radiated outside of the device. This effect could be minimized using headless screws that are completely buried in the threaded hole. Nevertheless, as it is shown in the figure, the gain loss is not very big even with conventional screws (which were the only ones available when the prototype was characterized).

Finally, the magnitude of the measured S_{11} parameter for different scanning directions can be found in Fig. 11.

TABLE 3. Comparison of some characteristics of the array implemented in this work with other works in the state of the art.

Parameter	This work	[4]	[10]	[5]	[14]	[18]
Number of radiating elements	4	64*	16**	4	16**	20
Maximum measured gain (dB)	12.0	17.0	8	11	10.7	19.1
Scanning range (°)	50	120***	50***	90	40***	14
Δ_{BW} (%) @12dB	23.5	5.6	9.7	12.8	9.0	4.3
Central frequency (GHz)	17	5.4	12.4	5.5	28	9.35
Power losses (dB)	0.46	4.2	11.1	1.5	8.50	0.73
Technology	Waveguide	Planar	Planar (BST)	SIW	Waveguide + Planar	Waveguide
Tuning method	Mechanical	Electronic	Electronic	Electronic	Electronic	Mechanical
Complexity	Medium	Medium	High	Medium	High	Medium

*Two-dimensional 8x8 array.
**Two-dimensional 4x4 array.
***The main lobe can be scanned both in azimuth and elevation.
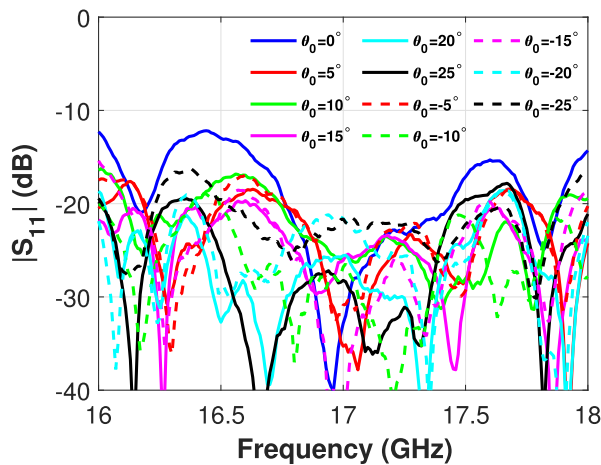

FIGURE 11. Measured magnitude of the S_{11} parameter of the complete antenna array for different scanning directions θ_0.

For $\theta_0 = 0°$ it is similar to that measured for the array without phase shifters which, as it happened with the radiation pattern measurements, is in accordance with the measured scattering parameters of the phase shifter. Moreover, for scanning directions other than $\theta_0 = 0°$ the S_{11} level is slightly improved. This can be explained by the partial cancellation of internal reflections in the CWFN due to the phase shift of each element, which does not occur for $\theta_0 = 0°$ since all the unitary elements are excited with the same phase and therefore the wave reflected by each of them towards the CWFN also has the same phase.

Relevant figures of merit for the reconfigurable phased array are the beam scanning range and the operation bandwidth. It is worth mentioning that the operation bandwidth does not only depend on the return loss level over the frequency band but also on the stability of the radiation pattern over this same band. In order to put the presented design in perspective, Table 3 compares it with other works by other authors in the state of the art. The works selected for this comparison represent the different available technological options for implementing reconfigurable phased arrays: pure planar implementation, pure waveguide implementation (like in the present work) and a hybrid of waveguide and planar technology.

The transmitarray presented in [4] consists of two 8×8 arrays of patch antennas. Each unit cell of one array is connected to its corresponding cell of the other array through a tunable reflection-type phase shifter like the one used in this work but implemented in planar technology. In [4] the reconfiguration of the phase shifter is achieved thanks to the use of varactor diodes. The main lobe of the radiation pattern can be scanned in the $\pm 60°$ range both in the azimuth and elevation planes since the array is two-dimensional. However, it should be noted that the varactor diodes present relatively high insertion losses (in comparison with a waveguide phase shifter) which have a certain impact on the efficiency of the antenna.

As shown in [10], the use of functional materials like the barium–strontium–titanate (BST) allows to achieve higher operation frequencies than planar designs based on varactors like [4], [5]. However, since these designs are based on an experimental technology the achieved scanning range is lower than the one provided by other planar alternatives, while the power losses are relatively high (being indeed the highest of all the presented works).

A SIW linear array is presented in [5]. In this design the phase shift between the array elements is obtained by means of reflection type phase shifters based on the use of varactor diodes, as in [4]. The SIW implementation seems to produce a certain improvement on the power losses and bandwidth performance over other planar designs, although the obtained values are not as good as those obtained by conventional waveguide implementations.

Another two-dimensional array is presented in [14], although in this case it is formed by a 4 × 4 array of horn antennas which are excited, with equal amplitude and phase, by a waveguide feeding network. This network incorporates one integrated circuit phase shifter to control the excitation phase of each horn electronically. The achieved beam scanning range is similar to the value obtained in this work. However, as it happened in [4] the use of tunable electronic components increases the power losses in comparison with a full waveguide implementation. Nevertheless it should be mentioned that, despite their high power losses, electronically reconfigurable arrays allow for a faster reconfiguration and a more compact implementation than mechanically reconfigurable waveguide arrays. Therefore, depending on the specific application requirements one option may result more appropriate than the other.

A different approach of a waveguide array with mechanical reconfiguration is presented in [18]. A linear array of radiating slots fed in series is present but instead of using tunable phase shifters to adjust the phase of the unit elements, the reconfigurability is achieved thanks to two rotating dielectric slabs inserted into the waveguide. Nevertheless, as it can be appreciated in the table, the achieved scanning range and bandwidth is lower than the one achieved by the proposed design based on waveguide reflection-type phase shifter.

In summary, the scanning range achieved in the present work is similar [14] or even better [18] than other state-of-the-art waveguide based designs. Additionally, the achieved bandwidth is superior than the one achieved by these designs thanks to the avoidance of electronic and resonant structures. This greater bandwidth is not only reflected on the return losses but also on the stability of the beam scanning over the operation frequency band, as shown in Fig. 9. Additionally, thanks again to the avoidance of electronic and dielectric tuning elements, the proposed design achieves a higher efficiency than other waveguide array designs in the state of the art [14], [18].

V. CONCLUSION
In this work, a reconfigurable phased array in waveguide technology has been presented. It is based on a novel reconfigurable reflection-type phase shifter which is controlled by means of two tuning screws, and that can be integrated with other shifters into a seamless module. The implementation in waveguide technology without introducing tunable electronic elements allows to reduce significantly the insertion losses in comparison with other more conventional implementations based on planar circuitry, achieving a high efficiency.

The reconfigurable phase shifter is manufactured in a single part by DMLS, avoiding misalignment and electric contact problems associated to multipart devices which can degrade the performance of the device.

The experimental results show that the main lobe of the radiation pattern can be effectively scanned between $\theta_0 = -25°$ and $\theta_0 = 25°$ and that the antenna is well matched for all these scanning directions, with a $|S_{11}|$ level below -12dB, achieving a greater bandwidth than other state of the art reconfigurable array designs.

REFERENCES
[1] P. Lotfi, S. Soltani, and R. D. Murch, "Printed endfire beam-steerable pixel antenna," *IEEE Trans. Antennas Propag.*, vol. 65, no. 8, pp. 3913–3923, Aug. 2017.

[2] S. Xiao, C. Zheng, M. Li, J. Xiong, and B.-Z. Wang, "Varactor-loaded pattern reconfigurable array for wide-angle scanning with low gain fluctuation," *IEEE Trans. Antennas Propag.*, vol. 63, no. 5, pp. 2364–2369, May 2015.

[3] P. Padilla, J. F. Valenzuela-Valdes, J. L. Padilla, J. M. Fernandez-Gonzalez, and M. Sierra-Castaner, "Electronically reconfigurable reflective phase shifter for circularly polarized reflectarray systems," *IEEE Microw. Wireless Compon. Lett.*, vol. 26, no. 9, pp. 705–707, Sep. 2016.

[4] C. Huang, W. Pan, X. Ma, B. Zhao, J. Cui, and X. Luo, "Using reconfigurable transmitarray to achieve beam-steering and polarization manipulation applications," *IEEE Trans. Antennas Propag.*, vol. 63, no. 11, pp. 4801–4810, Nov. 2015.

[5] Y. Ji, L. Ge, J. Wang, Q. Chen, W. Wu, and Y. Li, "Reconfigurable phased-array antenna using continuously tunable substrate integrated waveguide phase shifter," *IEEE Trans. Antennas Propag.*, vol. 67, no. 11, pp. 6894–6908, Nov. 2019.

[6] P. Sanchez-Olivares, P. P. Sanchez-Dancausa, and J. L. Masa-Campos, "Circularly conformal patch array antenna with omnidirectional or electronically switched directive beam," *IET Microw., Antennas Propag.*, vol. 11, no. 15, pp. 2253–2259, Dec. 2017.

[7] E. Garcia-Marin, P. Sanchez-Olivares, J. Herranz-Alpanseque, A. J. Martin-Trueba, J. L. Masa-Campos, and J. Corcoles, "Electronically reconfigurable microstrip array antenna with reflective phase shifters at ku band," in *Proc. 12th Eur. Conf. Antennas Propag. (EuCAP)*, 2018, pp. 1–5.

[8] L. Huitema, A. Ghalem, H. Wong, and A. Crunteanu, "Overview on functional materials for frequency tunable antennas," in *Proc. IEEE Conf. Antenna Meas. Appl. (CAMA)*, Sep. 2018, pp. 1–4.

[9] H. Wong, Q.-Y. Guo, A. Crunteanu, and L. Huitema, "A MMW reconfigurable antenna with switched beams using functional materials," in *Proc. 13th Eur. Conf. Antennas Propag. (EuCAP)*, Mar./Apr. 2019, pp. 1–3.

[10] M. Nikfalazar, M. Sazegar, A. Mehmood, A. Wiens, A. Friederich, H. Maune, J. R. Binder, and R. Jakoby, "Two-dimensional beam-steering phased-array antenna with compact tunable phase shifter based on BST thick films," *IEEE Antennas Wireless Propag. Lett.*, vol. 16, pp. 585–588, 2017.

[11] A. Ghalem, M. Rammal, L. Huitema, A. Crunteanu, V. Madrangeas, P. Dutheil, F. Dumas-Bouchiat, P. Marchet, C. Champeaux, L. Trupina, L. Nedelcu, and M. G. Banciu, "Ultra-high tunability of $Ba_{(2/3)}Sr_{(1/3)}TiO_3$-based capacitors under low electric fields," *IEEE Microw. Wireless Compon. Lett.*, vol. 26, no. 7, pp. 504–506, Jul. 2016.

[12] U. Shah, T. Reck, H. Frid, C. Jung-Kubiak, G. Chattopadhyay, I. Mehdi, and J. Oberhammer, "A 500–750 GHz RF MEMS waveguide switch," *IEEE Trans. THz Sci. Technol.*, vol. 7, no. 3, pp. 326–334, May 2017.

[13] Y. Wang, J. Hu, and Y. Luo, "A terahertz tunable waveguide bandpass filter based on Bimorph microactuators," *IEEE Microw. Wireless Compon. Lett.*, vol. 29, no. 2, pp. 110–112, Feb. 2019.

[14] M. K. Leino, R. Montoya Moreno, J. Ala-Laurinaho, R. Valkonen, and V. Viikari, "Waveguide-based phased array with integrated element-specific electronics for 28 GHz," *IEEE Access*, vol. 7, pp. 90045–90054, 2019.

[15] R. Reese, E. Polat, H. Tesmer, J. Strobl, C. Schuster, M. Nickel, A. B. Granja, R. Jakoby, and H. Maune, "Liquid crystal based dielectric waveguide phase shifters for phased arrays at W-Band," *IEEE Access*, vol. 7, pp. 127032–127041, 2019.

[16] S. M. Amin Momeni Hasan Abadi, J. H. Booske, and N. Behdad, "Exploiting mechanical flexure as a means of tuning the responses of large-scale periodic structures," *IEEE Trans. Antennas Propag.*, vol. 64, no. 3, pp. 933–943, Mar. 2016.

[17] A. Jouade, M. Himdi, A. Chauloux, and F. Colombel, "Mechanically pattern-reconfigurable bended horn antenna for high-power applications," *IEEE Antennas Wireless Propag. Lett.*, vol. 16, pp. 457–460, 2017.

[18] A. Ghasemi and J.-J. Laurin, "A continuous beam steering slotted waveguide antenna using rotating dielectric slabs," *IEEE Trans. Antennas Propag.*, vol. 67, no. 10, pp. 6362–6370, Oct. 2019.

[19] G. Matthaei, L. Young, and E. Jones, *Microwave Filters, Impedance-Matching Networks, and Coupling Structures* (Artech House Microwave Library). Norwood, MA, USA: Artech House, 1980.

[20] H.-W. Yao, K. A. Zaki, A. E. Atia, and R. Hershtig, "Full wave modeling of conducting posts in rectangular waveguides and its applications to slot coupled combline filters," *IEEE Trans. Microw. Theory Techn.*, vol. 43, no. 12, pp. 2824–2830, Dec. 1995.

[21] J. A. Ruiz-Cruz, M. M. Fahmi, and R. R. Mansour, "Generalized multiport waveguide switches based on multiple short-circuit loads in power-divider junctions," *IEEE Trans. Microw. Theory Techn.*, vol. 59, no. 12, pp. 3347–3355, Dec. 2011.

[22] P. Sanchez-Olivares and J. L. Masa-Campos, "Mechanically reconfigurable conformal array antenna fed by radial waveguide divider with tuning screws," *IEEE Trans. Antennas Propag.*, vol. 65, no. 9, pp. 4886–4890, Sep. 2017.

[23] P. Sanchez-Olivares, J. L. Masa-Campos, and J. Hernandez-Ortega, "Mechanical technique to customize a waveguide-slot radiating performance," *IEEE Trans. Antennas Propag.*, vol. 66, no. 1, pp. 426–431, Jan. 2018.

[24] P. Sanchez-Olivares, J. L. Masa-Campos, A. T. Muriel-Barrado, R. Villena-Medina, and G. M. Fernandez-Romero, "Mechanically reconfigurable linear array antenna fed by a tunable corporate waveguide network with tuning screws," *IEEE Antennas Wireless Propag. Lett.*, vol. 17, no. 8, pp. 1430–1434, Aug. 2018.

[25] "The European table of frequency allocations and applications in the frequency range 8.3 KHz to 3000 GHz," in *Proc. Eur. Conf. Postal Telecommun. Admin. (CEPT)*, Mar. 2019. [Online]. Available: https://www.efis.dk/sitecontent.jsp?sitecontent=ecatable

[26] A. T. Muriel-Barrado, J. L. Masa-Campos, and P. Sanchez-Olivares, "H-plane corporate waveguide-fed 4-aperture-stacked circular microstrip patch linear array for ku band applications," *Microw. Opt. Technol. Lett.*, vol. 59, no. 9, pp. 2216–2223, Sep. 2017.

[27] P. Kumar and J. L. Masa-Campos, "Waveguide fed circular microstrip patch antenna for ku band applications," *Microw. Opt. Technol. Lett.*, vol. 57, no. 3, pp. 585–589, Mar. 2015.

[28] J. A. Ruiz-Cruz, M. M. Fahmi, S. A. Fouladi, and R. R. Mansour, "Waveguide antenna feeders with integrated reconfigurable dual circular polarization," *IEEE Trans. Microw. Theory Techn.*, vol. 59, no. 12, pp. 3365–3374, Dec. 2011.

[29] S. Fouladi, F. Huang, W. D. Yan, and R. R. Mansour, "High-*Q* narrowband tunable combline bandpass filters using MEMS capacitor banks and piezomotors," *IEEE Trans. Microw. Theory Techn.*, vol. 61, no. 1, pp. 393–402, Jan. 2013.

[30] D. M. Pozar, *Microwave Engineering*, 4th ed. Hoboken, NJ, USA: Wiley, 2011.

[31] R. V. Garver, "Broad-band diode phase shifters," *IEEE Trans. Microw. Theory Techn.*, vol. MTT-20, no. 5, pp. 314–323, May 1972.

[32] L. Polo-López, J. L. Masa-Campos, and J. A. Ruiz-Cruz, "Reconfigurable H-plane waveguide phase shifters prototyping with additive manufacturing at K-band," *Int. J. RF Microw. Comput.-Aided Eng.*, vol. 29, no. 12, pp. 1–10, Dec. 2019.

[33] C. Koenen, U. Siart, T. F. Eibert, and G. D. Conway, "A self-aligning cylindrical sliding short plunger for millimeter-wave rectangular waveguides and its application in a reflection-type phase shifter," *IEEE Trans. Microw. Theory Techn.*, vol. 65, no. 2, pp. 449–458, Feb. 2017.

[34] H. Riblet, "The short-slot hybrid junction," *Proc. IRE*, vol. 40, no. 2, pp. 180–184, Feb. 1952.

[35] J. A. Ruiz-Cruz, J. R. Montejo-Garai, and J. M. Rebollar, "Short-slot E- and H-plane waveguide couplers with an arbitrary power division ratio," *Int. J. Electron.*, vol. 98, no. 1, pp. 11–24, Jan. 2011.

[36] Y. Zhang, Q. Wang, and H. Xin, "A compact 3 dB E-plane waveguide directional coupler with full bandwidth," *IEEE Microw. Wireless Compon. Lett.*, vol. 24, no. 4, pp. 227–229, Apr. 2014.

[37] Z. Chen, S.-G. Zhou, and T.-H. Chio, "A class of all metal cavity-backed slot array with direct metal laser sintering," *IEEE Access*, vol. 6, pp. 69650–69659, 2018.

[38] R. Shavit, L. Pazin, Y. Israeli, M. Sigalov, and Y. Leviatan, "Dual frequency and dual circular polarization microstrip nonresonant array pin-fed from a radial line," *IEEE Trans. Antennas Propag.*, vol. 53, no. 12, pp. 3897–3905, Dec. 2005.

[39] L. Pazin and Y. Leviatan, "Uniform amplitude excitation of radiating elements in array antenna pin-fed from radial waveguide," *IEE Proc.-Microw., Antennas Propag.*, vol. 148, no. 6, pp. 413–417, Dec. 2001.

LUCAS POLO-LÓPEZ received the B.Sc. and M.Sc. degrees in telecommunication engineering from the Universidad Autónoma de Madrid, Madrid, Spain, in 2014 and 2016, respectively, where he is currently pursuing the Ph.D. degree.

Since 2015, he has been with the Radiofrequency Circuits, Antennas, and Systems (RFCAS) Group, Universidad Autónoma de Madrid. His current research interests include the computer-aided design of horn antennas and passive waveguide devices, as well as the application of additive manufacturing techniques to the construction of waveguide devices.

JOSÉ LUIS MASA-CAMPOS was born in Madrid, Spain, in 1974. He received the master's and Ph.D. degrees from the Universidad Politécnica de Madrid, Spain, in 1999 and 2006, respectively.

From 1990 to 2003, he developed his professional activity in the Research and Development Department, Company RYMSA with the design of base station antennas for mobile communications and satellite antennas. From 2002 to 2003, he directed the Research and Development Department, RYMSA. From 2003 to 2007, he worked as Researcher with Universidad Politécnica de Madrid, and in 2005, he joined the Radiofrequency Group (RFCAS), Universidad Autónoma de Madrid, as an Associate Professor. His main current research interests are in active and passive planar array antennas (microstrip, substrate integrated waveguide or metallic waveguide technologies), associated antenna feeding networks, and new additive manufacturing techniques applied to microwave circuits and antennas

ALFONSO TOMÁS MURIEL-BARRADO was born in Madrid, Spain, in 1990. He received the M.Sc. degree in telecommunication engineering from the Universidad Autónoma de Madrid (UAM), Spain, in 2015. He is currently pursuing the Ph.D. degree from the Universidad Politécnica de Madrid (UPM).

In February 2020, he joined UAM as an Associate Professor. He is also a part of the Grupo de Radiación (GR) Research Group, UPM. His current research interests include design and prototyping of planar array antennas in different technologies as well as their migration to beam-steered systems by means of different radiofrequency/microwave circuitry.

PABLO SANCHEZ-OLIVARES was born in Madrid, Spain, in 1987. He received the degree in telecommunication engineering and the Ph.D. degree from the Universidad Autonoma de Madrid (UAM), Spain, in 2011 and 2018, respectively.

From 2018 to 2019, he was worked as an Adjunct Professor with UAM, as well as a Postdoctoral Researcher Associate with the Universidad de Alcalá de Henares (UAH). Since 2019, he has been an Assistant Professor with the Universidad Politécnica de Madrid (UPM). His current research interests are based on the design, manufacturing and measurement of planar array antennas, phased array antennas, and waveguide antennas.

JUAN CÓRCOLES (Senior Member, IEEE) was born in Albacete, Spain, in 1981. He received the Ingeniero de Telecomunicación degree (the B.Sc. and M.Sc. degrees in electrical engineering) and the Doctor Ingeniero de Telecomunicación degree (the Ph.D. degree in electrical engineering) from the Universidad Politécnica de Madrid, Spain, in 2004 and 2009, respectively, the Diplomado en Ciencias Empresariales degree (the B.Sc. degree in business science) from the Universidad Complutense de Madrid, in 2008, and the Licenciado en Economía degree (the M.Sc. degree in Economics) from the Universidad Nacional de Educación a Distancia, Madrid, Spain, in 2010.

He was a Visiting Researcher with the Institut für Hochfrequenztechnik und Elektronik (IHE), Universität Karlsruhe (TH), Germany, from November 2008 to March 2009, IT'IS Foundation, ETHZ, Zurich, Switzerland, from July 2013 to September 2013 and June 2016 and August 2016, and King's College London, U.K., from October 2018 to December 2018. Since 2010, he has been with the Universidad Autónoma de Madrid, Spain, where he became an Associate Professor, in 2015. His current research interests include the development and application of computational methods and optimization techniques to the analysis and design of microwave circuits and antennas, especially antenna arrays, as well as medical and other novel applications of radiofrequency electromagnetic fields.

EDUARDO GARCIA-MARIN received the M.Sc. degree in telecommunication engineering from the Universidad Autónoma de Madrid (UAM), Spain, in 2016, where he is currently pursuing the Ph.D. degree.

His current research interest is in passive and active array antennas and evaluation of different manufacturing techniques applied to antennas.

JORGE A. RUIZ-CRUZ (Senior Member, IEEE) received the Ingeniero de Telecomunicación degree and the Ph.D. degree from the Universidad Politécnica de Madrid, Madrid, Spain, in 1999 and 2005, respectively.

Since 2006, he has been with the Universidad Autónoma de Madrid, Madrid, where he became an Associate Professor, in 2009. His current research interests include the computer aided design of microwave passive devices and circuits (filters, multiplexers, and orthomodes).

• • •